

# Dynamic Whole-Arm Dexterous Manipulation In The Plane

S.L. Yeap  
Dept. of CS  
syeap@cs.tamu.edu

J.C. Trinkle  
Dept. of CS  
trink@cs.tamu.edu

Texas A&M University, College Station, TX 77843-3112

## Abstract

A dynamic model of a dexterous manipulation system can be used for predicting the feasibility of a manipulation plan generated under the quasistatic assumption but executed under dynamic conditions. Contact forces between the object and manipulator are calculated to determine whether contacts can be maintained for the planned motion. Compressive contact forces indicate that contacts can be maintained for the specified manipulation plan and this implies that actual dynamic manipulation succeeds. Results of the solution of dynamic equations are given for selected objects and video images of successful plans are shown.

## 1 Introduction

Dexterous manipulation involves the set of motions required to grasp an object in a robot hand and change its position and orientation through a series of coordinated motions. It is related to robot motion planning in the sense of planning the trajectories of the manipulator joints and object position and orientation. Dexterous manipulation differs from other types of robotic manipulation in that the object being grasped can also be repositioned and reoriented within the end-effector while the end-effector itself is undergoing translation and rotation.

Most research has focused on the kinematics and dynamics of fingertip-only dexterous manipulation [2, 5, 12, 1]. As for whole-arm manipulation (which aims to use all surfaces of the hand) the quasistatic assumption has often been applied. Early work by Trinkle [7, 9] described lifting a polygon using an enveloping grasp with sliding contacts. Later work by Trinkle and Hunter [8] investigated the search for a manipulation plan of a frictionless polygon acted upon by a palm and two fingers. The quasistatic assumption was maintained and contacts were allowed between finger edges and tips with object.

This paper describes whole-arm manipulation that takes into account the dynamics of the hand and object during manipulation. In particular, it will show that it is possible to predict whether a quasistatic manipulation plan will succeed when executed dynam-

cally.

## 2 Dynamics of whole-arm manipulation

We will study the motion of a manipulator consisting of two single-link fingers in contact with a polygonal object. Each link has a revolute joint. Fig. 1 shows the manipulator and its associated parameters.

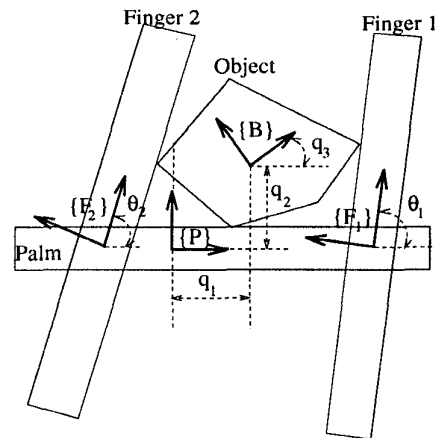


Figure 1: Dexterous manipulator configuration

The dynamic equation at joint  $i$  ( $i = \{1, 2\}$ ) relating the actuator torque to the joint acceleration, velocity, and position is

$$\tau_i = J_i \ddot{\theta}_i + B_i \dot{\theta}_i + D_i \text{sgn}(\dot{\theta}_i) + \dot{\mathbf{J}}_{in}^T \mathbf{c}_n + \dot{\mathbf{J}}_{it}^T \mathbf{c}_t \quad (1)$$

where  $\mathbf{c}_n$  is the vector of normal wrench intensities, and  $\mathbf{c}_t$  is the vector of tangential wrench intensities.  $J_i$ ,  $\tau_i$ ,  $\theta_i$ ,  $\dot{\theta}_i$ ,  $\ddot{\theta}_i$ , are referred to the output side of the respective actuators.  $J_i$  is the combined moment of inertia at joint  $i$  due to the dc motor, harmonic drive gearing, flexible coupling, and the link.  $\tau_i$  is the torque generated at joint  $i$ ,  $B_i$  is the viscous friction

coefficient,  $D_i$  is the dry friction coefficient.  $\mathbf{j}_{in}$  is the Jacobian vector of the  $i$ -th joint.

The dynamic equation of the object being manipulated is

$$\mathbf{M}\ddot{\mathbf{q}} = \mathbf{g}_{obj} + \mathbf{W}_n \mathbf{c}_n + \mathbf{W}_t \mathbf{c}_t \quad (2)$$

$\mathbf{M}$  is the diagonal 3x3 mass and moment of inertia matrix.  $\ddot{\mathbf{q}}$  is a three-dimensional vector giving the object's acceleration.  $\mathbf{g}_{obj}$  is the external wrench, and in our case consists only of the gravitational wrench due to the object's weight.  $\mathbf{W}_n$  and  $\mathbf{W}_t$  are the normal and tangential wrench matrices respectively defined in [11]. For planar manipulation,  $\mathbf{W}_n$  and  $\mathbf{W}_t$  have 3 rows and their numbers of columns are equal to the number of contacts.  $\mathbf{c}_n$  and  $\mathbf{c}_t$  are the vectors of normal and tangential wrench intensities respectively and the number of elements in each is equal to the number of contacts. When the contacts are all sliding, the tangential wrench intensity can be expressed in terms of the normal wrench intensity as:

$$\mathbf{c}_t = -\mathbf{U}\Xi \mathbf{c}_n \quad (3)$$

where  $\Xi$  and  $\mathbf{U}$  are as defined in [11].  $\mathbf{U}$  is a matrix whose diagonal elements are the coefficients of friction between the object and the manipulator and all off-diagonal elements are zero.  $\Xi$  is also a diagonal matrix; the diagonal elements are either +1 or -1 and indicate the direction of sliding.

Our goal is to solve the dynamic equations under the initial condition that we have 4 sliding contacts. Assuming that all bodies are rigid, the kinematic constraint for bodies moving with sliding contacts to maintain contact is expressed as the following equation:

$$\mathbf{W}_n^T \dot{\mathbf{q}} = \mathcal{J}_n \dot{\boldsymbol{\theta}} \quad (4)$$

$\mathcal{J}_n$  is the normal Jacobian matrix that maps the joint velocities to the normal component of velocities at the contact points. Each row of the left-hand side is the normal component of the velocity of a contact point on the object being manipulated and the right-hand side is the velocity of the contact point on the link. This equation says that two moving objects can only maintain contact if they have the same velocity in the contact normal direction.

Let us consider the case of 4 sliding contacts. In this case,  $\mathbf{W}_n$  is a 3x4 matrix. The Jacobian matrix,  $\mathcal{J}_n$ , is 4x2 corresponding to 4 contacts and 2 joints. Both of these quantities are defined in [11]. When the Jacobian matrix is partitioned into 2 columns, we can write  $\mathcal{J}_n$  as:

$$\mathcal{J}_n = [ \mathbf{j}_{1n} \quad \mathbf{j}_{2n} ] \quad (5)$$

## 2.1 Velocities and accelerations derived from the kinematic constraint

For velocities, we specify  $\dot{\theta}_1$  and solve for  $\dot{\mathbf{q}}$  and  $\dot{\theta}_2$ . To do this, we partition the matrix

$$[ \mathbf{W}_n^T \quad -\mathcal{J}_n ]$$

into

$$[ \mathbf{W}_n^T \quad -\mathbf{j}_{2n} \quad | \quad -\mathbf{j}_{1n} ] \quad .$$

Following the notation in [11], let us make the following definitions:

$$\mathbf{P}_{A_I} \triangleq [ \mathbf{W}_n^T \quad -\mathbf{j}_{2n} ] \quad \text{and} \quad \mathbf{P}_{A_{II}} \triangleq -\mathbf{j}_{1n}, \quad (6)$$

where  $\mathbf{P}_{A_I}$  is nonsingular. If  $\mathbf{P}_{A_I}$  cannot be defined so that it is nonsingular, then the rest of the derivations would have to make use of the pseudoinverse of  $\mathbf{P}_{A_I}$  rather than the inverse. We can then write:

$$[ \mathbf{P}_{A_I} \quad \mathbf{P}_{A_{II}} ] \begin{bmatrix} \dot{\mathbf{q}} \\ \dot{\theta}_2 \\ \dot{\theta}_1 \end{bmatrix} = \mathbf{0} \quad , \quad (7)$$

where  $\mathbf{0}$  is the zero vector of length 5. This leads us to:

$$\mathbf{P}_{A_I} \begin{bmatrix} \dot{\mathbf{q}} \\ \dot{\theta}_2 \end{bmatrix} = -\mathbf{P}_{A_{II}} \dot{\theta}_1 \quad , \quad (8)$$

thereby allowing us to obtain  $\dot{\mathbf{q}}$  and  $\dot{\theta}_2$  through the inversion of  $\mathbf{P}_{A_I}$  as follows:

$$\begin{bmatrix} \dot{\mathbf{q}} \\ \dot{\theta}_2 \end{bmatrix} = -\mathbf{P}_{A_I}^{-1} \mathbf{P}_{A_{II}} \dot{\theta}_1 \quad . \quad (9)$$

Note that  $\mathbf{P}_{A_I}$  and  $\mathbf{P}_{A_{II}}$  are dependent on  $\boldsymbol{\theta}$  and  $\mathbf{q}$ . Since we are dealing with a 5 degree of freedom system and we have 4 sliding contacts, there is 1 degree of freedom remaining and we can specify its desired value. Specifying the desired value of  $\theta_1$ , we can obtain numerical values for  $\theta_2$  and  $\mathbf{q}$  and hence the elements of the matrix  $\mathbf{P}_{A_I}$ . This is done by solving a set of simultaneous nonlinear equations, each of which is a C-function equated to zero. C-functions, which are widely used in robot motion planning [4], describe the position and orientation of a robot relative to an object or obstacle. A similar reasoning applies to  $\mathbf{P}_{A_{II}}$ . Equation (9) allows us to obtain  $\dot{\mathbf{q}}$  and  $\dot{\theta}_2$  once we know the configuration parameters  $\theta_1$ ,  $\theta_2$ ,  $\mathbf{q}$ , and joint 1 velocity  $\dot{\theta}_1$ . By differentiating equation (9) with respect to time, we obtain the accelerations of the object and joint 2 in terms of the velocity and acceleration of joint 1.

The above analysis deals with sliding contacts only. The same analysis can be done if rolling contacts are present (but which are not considered in this paper). The number of contact constraints will then be  $2R+S$  where  $R$  is the number of rolling contacts and  $S$  is the number of sliding contacts. This also determines the dimension of the  $\mathbf{P}_{A_I}$  matrix. Detailed consideration of this analysis can be found in [11].

## 2.2 Derivation of the differential equation of motion

At this time, recall equation (2) and the dynamic equation for finger 2 as given by equation (1) which we shall rewrite as follows:

$$\mathbf{M}\ddot{\mathbf{q}} - \mathbf{g}_{\text{obj}} - \mathbf{W}_n \mathbf{c}_n - \mathbf{W}_t \mathbf{c}_t = \mathbf{0} , \quad (10)$$

$$\mathbf{J}_2 \ddot{\theta}_2 + \mathbf{B}_2 \dot{\theta}_2 + \mathbf{D}_2 \text{sgn}(\dot{\theta}_2) + \mathbf{j}_{2n}^T \mathbf{c}_n + \mathbf{j}_{2t}^T \mathbf{c}_t = \tau_2 . \quad (11)$$

Equation (10) gives the dynamics for the object and equation (11) gives the dynamics for finger 2.  $\mathbf{c}_t$  can be expressed in terms of  $\mathbf{c}_n$  by using equation (3). Thus,

$$\mathbf{W}_n \mathbf{c}_n + \mathbf{W}_t \mathbf{c}_t = [\mathbf{W}_n - \mathbf{W}_t \mathbf{U}\Xi] \mathbf{c}_n , \quad (12)$$

$$\mathbf{j}_{2n}^T \mathbf{c}_n + \mathbf{j}_{2t}^T \mathbf{c}_t = [\mathbf{j}_{2n}^T - \mathbf{j}_{2t}^T \mathbf{U}\Xi] \mathbf{c}_n . \quad (13)$$

Let

$$\mathbf{W}_{A\mu} = [\mathbf{W}_n - \mathbf{W}_t \mathbf{U}\Xi] , \quad (14)$$

$$\mathbf{j}_{2A\mu}^T = [\mathbf{j}_{2n}^T - \mathbf{j}_{2t}^T \mathbf{U}\Xi] . \quad (15)$$

The complete dynamic equations of the system can therefore be obtained by substituting for  $\ddot{\mathbf{q}}$ ,  $\ddot{\theta}_2$  and  $\dot{\theta}_2$ . The differential equation can be expressed as:

$$\Phi_1 \ddot{\theta}_1 + \Phi_2 \dot{\theta}_1 + \Phi_3 = 0 , \quad (16)$$

where  $\Phi_1$ ,  $\Phi_2$ , and  $\Phi_3$  are coefficients dependent on the configuration parameters and their first time derivatives. The solution to this differential equation is the time trajectory of  $\theta_1$ . To guarantee that the 4 contacts are maintained, we must check that  $\mathbf{c}_n > 0$ .

Given the initial value of  $\theta_1$ , we can solve the set of four nonlinear C-functions to obtain the values of  $\theta_2$  and  $\mathbf{q}$ . With these values, we can form the normal wrench and Jacobian matrices. As time progresses, the value of  $\theta_1$  changes and hence the values of  $\theta_2$  and  $\mathbf{q}$ .  $\Phi_1$ ,  $\Phi_2$ , and  $\Phi_3$  are updated every time interval of the differential equation solver.

At each time step, we solve equation (16) to obtain the values of  $\theta_1$ ,  $\dot{\theta}_1$ , and  $\ddot{\theta}_1$ . From these, the values for joint 2 can also be obtained from the kinematic constraints. The normal component of each contact force  $c_{in}$  is then computed and the sign indicates whether the  $i$ -th contact force is compressive or tensile. If  $c_{in}$  is positive, then we know that for the particular time step, contact is maintained between an object feature and a link feature. If a set of contacts (known as contact formation) is maintained, then we know that motion is possible for that contact formation.

The dynamics code is implemented in the C language and runs on an IBM RS/6000 workstation. Function calls are made to the IMSL library to numerically solve systems of nonlinear equations, perform matrix computations, and numerically solve the differential equation.

## 3 Experimental procedure and results

We will select some manipulation plans for the polygons and investigate their dynamics and contact forces given torque trajectories for the joints. If the plans turn out to be feasible in simulation, we will execute them using the dexterous manipulator and verify that this is indeed so.

For our experiments, we have chosen to use an irregular heptagon and a hexagon. All the plans involve large scale reorientation of the objects. More specifically, they consist of sliding the object to the left and then trying to flip it rightwards over a vertex that is touching the palm. The sequence of finger and object motions for the irregular heptagon is the same as the quasistatic plan described in [10]. This is shown in Fig. 2. We are especially interested in showing that this plan works also in a dynamic environment given the torque trajectories that we applied. If this plan can be executed both in dynamic simulation and on the prototype dexterous manipulation system that we have in the laboratory, then we would have established the validity of the dynamic model being used.

### 3.1 Manipulation strategy

To manipulate the objects, our strategy is to apply a sequence of coordinated torques to the joints. We start off by choosing torque values for both joints, and use them in solving the dynamic equations. Contact forces are then calculated. If the contact forces turn out to be compressive, then we know that the object can maintain the set of contacts during motion. The object goes through several different contact formations during the course of manipulation. Therefore, we continue this process for different contact formations until the object gets into its final configuration. If the contact forces stay compressive all this time, then we have a feasible manipulation plan.

The method of finding the torque trajectories is empirical and relies on systematically increasing or decreasing the torque until the desired object motion is achieved and no contacts break. Given the torque values, the dynamic equations are used for simulating the motion and the contact force equation is used for checking the values of contact forces. The type of object motion encountered during manipulation consists only of sliding. To achieve sliding motion to the left, an anti-clockwise torque is applied to finger 1 (right finger). From [10], we have a good idea of the amount of torque required to bring about this motion. If applying this torque does not make the object slide to the left, the torque is increased by 10%. This process is continued until the object begins to slide. Thereafter, the torque is increased to make the object slide faster. When it is observed that the object edge is not in contact with the palm, the torque is decreased by 10% and the resulting torque is recorded as part of the trajectory. To make the object slide to the right, the reasoning is similar except that the torque is applied to finger 2. To make the object flip over to the right we apply a step jump in the torque of finger 2.

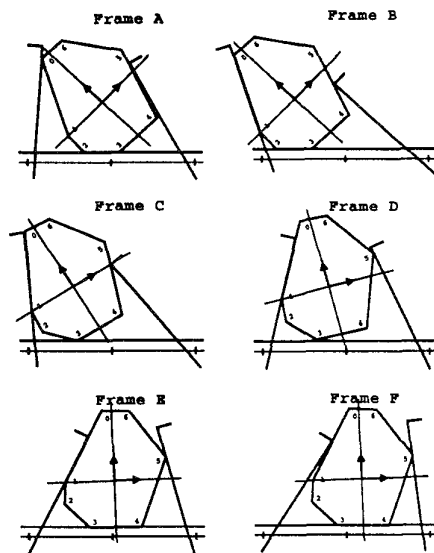


Figure 2: Irregular heptagon manipulation plan

Using the above guidelines, we were able to obtain torque trajectories for joints 1 and 2 ( Fig. 6 ) to manipulate the irregular heptagon with compressive contact forces. The results from dynamic simulation thus show that a quasistatic plan [10] corresponding to Fig. 2 can also work in a dynamic environment. With only slight modifications to the quasistatic torque trajectories for the irregular heptagon, we were able to obtain torque trajectories for the hexagon. This gives rise to the plan shown in Fig. 3.

Using the torque trajectories obtained in the previous section, we set out to see if we could actually obtain the desired manipulations. It turned out that we succeeded in manipulating the irregular heptagon and the hexagon as predicted. Figs. 4 and 5 show images of some of the frames taken from video recordings of the objects in motion. They show that the results agree with those predicted by the dynamic simulation.

#### 4 Conclusion and Future Research

We have derived the dynamic equations for a prototype dexterous manipulation system. A dynamic simulator was developed to predict whether contacts could be maintained under a specified motion plan.

Given candidate manipulation plans, we calculated the contact forces between manipulator and workpiece and selected those that were compressive. These plans were then executed on the dexterous manipulator and the plans succeeded for the irregular heptagon and the hexagon. We conclude that it is possible to predict the outcome of a quasistatic manipulation plan in a dynamic environment given the dynamic model of the system and torque trajectories. Possibilities for future work include incorporating tactile sensors on the finger surfaces, using a sensed-torque technique to

control the fingers during manipulation, and using a higher speed data acquisition board to read more sensors faster.

#### Acknowledgments

This research was supported in part by the National Science Foundation, grant no. IRI-9304734, the Texas Advanced Research Program, grant no. 999903-078, the Texas Advanced Technology Program, grant no. 999903-095, and NASA Johnson Space Center through the Universities' Space Automation and Robotics Consortium, contract no. 28920-32525. Any findings, conclusions, or recommendations expressed herein are those of the authors and do not necessarily reflect the views of the granting agencies.

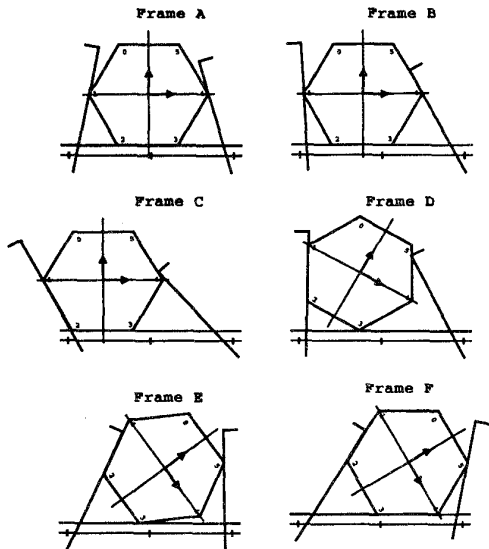


Figure 3: Hexagon manipulation plan

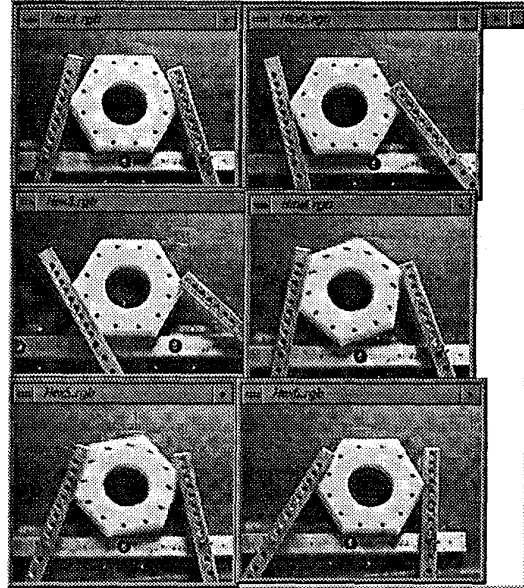


Figure 5: Video frames of hexagon manipulation sequence

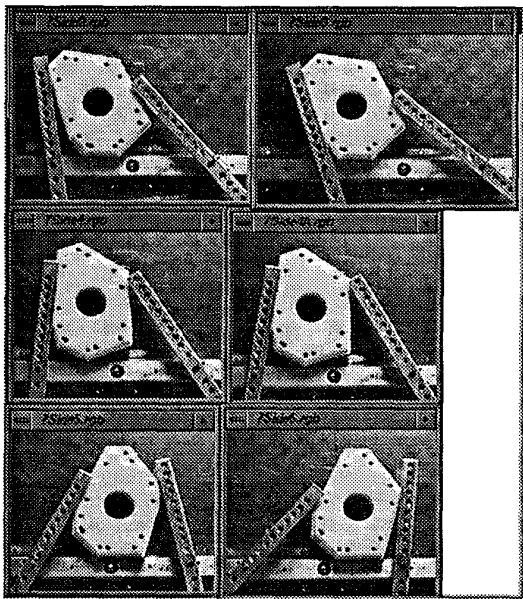


Figure 4: Video frames of irregular heptagon manipulation sequence

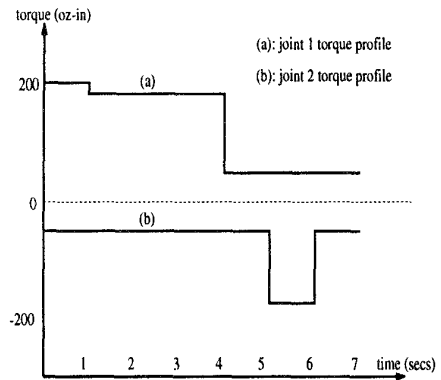


Figure 6: Torque trajectories for irregular heptagon

## References

- [1] A. Cole, P. Hsu, and S. Sastry, "Dynamic control of sliding by robot hands for regrasping," *IEEE Transactions on Robotics and Automation*, vol. 8, no. 1, pp. 42–52, February 1992.
- [2] R. S. Fearing, "Simplified grasping and manipulation with dextrous robot hands," *IEEE Journal of Robotics and Automation*, vol. RA-2, pp. 188–195, December 1986.
- [3] J. A. Kuzdrall, "Build an error-free encoder interface," *Electronic Design*, vol. 40, no. 19, pp. 81–87, Sept. 17, 1992.
- [4] J. C. Latombe, *Robot Motion Planning*. Norwell, Massachusetts: Kluwer Academic Publishers, 1991.
- [5] T. Okada, "Computer control of multijointed finger system for precise object-handling," *IEEE Transactions on Systems, Man, and Cybernetics*, vol. SMC-12, pp. 289–298, May/June 1982.
- [6] J. K. Salisbury, "Whole arm manipulation," in *Robotics Research : The Fourth International Symposium*, pp. 183–189, Santa Cruz, California, August 1987.
- [7] J. C. Trinkle, J. M. Abel, and R. P. Paul, "An investigation of frictionless, enveloping grasping in the plane," *International Journal of Robotics Research*, vol. 7, no. 3, pp. 33–51, June 1988.
- [8] J. C. Trinkle and J. J. Hunter, "A framework for planning dexterous manipulation," in *Proc. IEEE International Conference on Robotics and Automation*, pp. 1245–1251, Sacramento, California, April 1991.
- [9] J. C. Trinkle and R. P. Paul, "Planning for dexterous manipulation with sliding contacts," *International Journal of Robotics Research*, vol. 9, no. 3, pp. 24–48, June 1990.
- [10] J. C. Trinkle, R. C. Ram, A. O. Farahat, and P. F. Stiller, "Dexterous manipulation planning and execution of an enveloped slippery workpiece," in *Proc. IEEE International Conference on Robotics and Automation*, pp. 442–448, Atlanta, Georgia, May 1993.
- [11] J.C. Trinkle and D.C. Zeng, "Prediction of the quasistatic planar motion of a contacted rigid body," to appear in *IEEE Transactions on Robotics and Automation*, vol. RA-10, no. 6, 1994.
- [12] T. Yoshikawa and K. Nagai, "Manipulating and grasping forces in manipulation by multifingered robot hands," *IEEE Transactions on Robotics and Automation*, vol. 7, no. 1, pp. 67–77, February 1991.